

The Phase Diagram of $\text{NaNO}_3/\text{KNO}_3$

(submitted to *Thermochemica Acta*)

C. M. Kramer, C. J. Wilson

Prepared by Sandia Laboratories, Albuquerque, New Mexico 87185
and Livermore, California 94550 for the United States Department
of Energy under Contract DE-AC04-76DP00789.

Printed April 1980



Sandia Laboratories

Issued by Sandia Laboratories, operated for the United States Department of Energy by Sandia Corporation.

NOTICE

This report was prepared as an account of work sponsored by the United States Government. Neither the United States nor the United States Department of Energy, nor any of their employees, nor any of their contractors, subcontractors, or their employees, makes any warranty, express or implied, or assumes any legal liability or responsibility for the accuracy, completeness or usefulness of any information, apparatus, product or process disclosed, or represents that its use would not infringe privately owned rights.

SAND80-8502
Unlimited Release
Printed April 1980

THE PHASE DIAGRAM OF $\text{NaNO}_3/\text{KNO}_3$

C. M. Kramer
Exploratory Chemistry Division I

C. J. Wilson
Exploratory Chemistry Division II
Sandia National Laboratories, Livermore

ABSTRACT

The binary phase diagram of NaNO_3 and KNO_3 was studied using differential scanning calorimetry (DSC). The phase diagram was modeled with regular solution theory. By fitting the model to the minimum melting point of the system, the regular solution parameters and the heats of mixing for solid solutions of NaNO_3 and KNO_3 were estimated. Good agreement was obtained between our data for the liquidus, the previously determined liquidus, and the liquidus calculated from the model.

CONTENTS

	<u>Page</u>
Introduction	7
Experimental Technique	9
Experimental Results	10
Theory	16
Calculational Results and Comparison to Experiment	20
Conclusions	26
REFERENCES	29

ILLUSTRATIONS

<u>No.</u>		<u>Page</u>
1	Published phase diagrams of NaNO ₃ /KNO ₃	8
2	Schematic drawing of DSC peaks	11
3	Experimental data for NaNO ₃ /KNO ₃ phase diagram	12
4	Sketch of free energy curves for solid and liquid solutions	15
5	Schematic drawing of the equilibrium of a solid solution and a liquid solution	18
6	Calculated NaNO ₃ /KNO ₃ phase diagram and experimental data	21
7	Comparison of calculated and published NaNO ₃ /KNO ₃ phase diagrams	23
8	Comparison of calculated and published NaCl/KCl phase diagrams	25

TABLES

1	Tabulated DSC results	13
---	-----------------------	----

THE PHASE DIAGRAM OF $\text{NaNO}_3/\text{KNO}_3$

Introduction

Interest in sodium and potassium nitrate chemistry has been heightened in recent years because of the potential application to energy systems. For example, molten sodium and potassium nitrate mixtures have been proposed for use in solar large power plants, both as storage media and as the high-temperature heat transfer fluid.^{1,2} These salts and their mixtures have low melting points (<520 K) or low-temperature eutectics and are relatively non-corrosive, chemically stable, and inexpensive, all desirable characteristics for industrial fluids.

The $\text{NaNO}_3/\text{KNO}_3$ diagram, studied before by Berman and Berul³ and Kofler⁴ and reviewed by Voskresenskaya,⁵ is reported to be an isomorphous binary with a minimum melting point (see Figure 1). In the most recent study Kofler used a hot-stage-microscope technique to determine the solidus and liquidus. Berman and Berul, using polythermal-visual techniques, determined a liquidus that differed slightly (< 10 K) from that of Reference 4.

Recently, an increasing number of calculations have been performed to predict complex phase diagrams.^{6,7} Such calculations can often substitute for tedious and difficult experiments, and provide insight into the thermodynamic properties of these materials. We have completed our own experimental and theoretical investigation of the $\text{NaNO}_3/\text{KNO}_3$ phase diagram and report

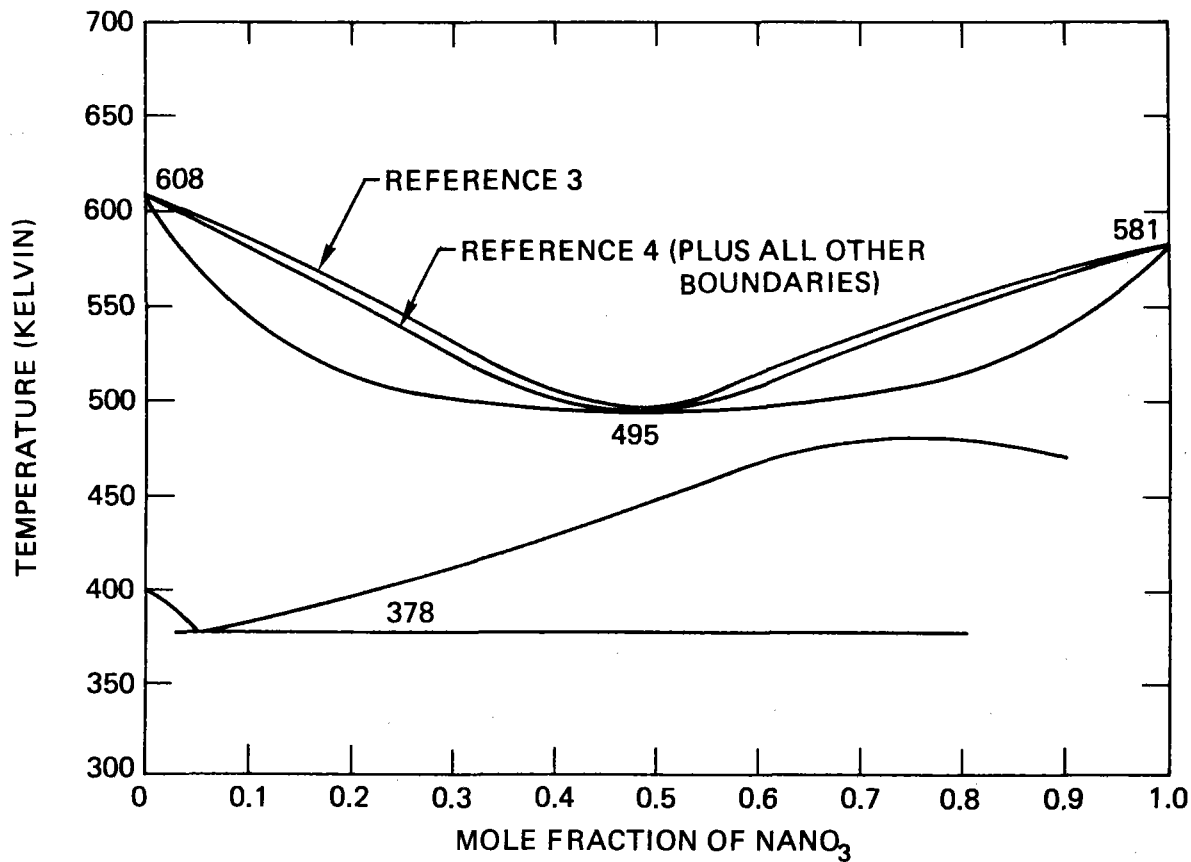


Fig. 1: Published phase diagrams of NaNO_3 - KNO_3

the results here. To predict the liquidus and solidus in the NaNO_3 - KNO_3 system we wrote a computer code based on a fundamental treatment of the thermodynamics of solutions. By comparing the calculated phase diagram with experimental data, obtained by differential scanning calorimetry, we gained insight into the behavior of nitrate salt solutions.

The remainder of this report is organized as follows: After briefly describing our experimental setup, we discuss the experimental results. The thermodynamic theory is then presented, following which the calculational results are compared with experiment.

Experimental Technique

A Perkin-Elmer differential scanning calorimeter (DSC-2) was used for all measurements. The DSC was calibrated with In and K_2CrO_4 (Perkin-Elmer standards), whose temperatures of fusion and solid-state transition, respectively, are well known. The salt samples were heated several times at constant heating rates and the thermal spectra of their melting behavior were recorded.

All our samples consisted of reagent-grade sodium nitrate and potassium nitrate, dried at 380 K under vacuum for at least 12 hours. Batches were prepared at 10 mole percent intervals and ground in a micromill to assure uniformity. For certain composition ranges to be studied in more detail, additional batches were prepared at 2 mole percent intervals. Small samples (< 20 mg) were encapsulated in high-pressure stainless steel holders or hermetically sealed in aluminum pans.

Experimental Results

A wide variety of DSC peak shapes were observed for the different $\text{NaNO}_3\text{-KNO}_3$ mixtures as illustrated in Figure 2. In many of the broad peaks, local maxima are observed. Because the peaks are not sharp and some had gradually changing slopes, we had to determine the most reliable method for reporting the liquidus and solidus determined from the numerous peak shapes. The shape of DSC peaks depends upon the purity and composition, thermal contact of the sample in the pan, sample pretreatment, the DSC operating parameters, and the thermal transition being studied.⁸ We made many DSC profiles of the salt mixtures using different heating rates (1.25-20 K/min), sample sizes (1-25 mg), sample pretreatment (prior grinding or fusion), and DSC energy scales (.5-5 mcal/sec) to find consistent results for the liquidus and solidus. We found that using highly sensitive energy scales and heating rates of 10 K/min or less produced results that could be easily duplicated.

The lowest and highest temperatures at which the DSC traces (of melting the salt samples) deviated from a straight base line were consistent from run to run and sample to sample. Therefore, the initial and final points of deviation from the base line were chosen as the solidus and liquidus temperatures for the samples. These are plotted as a phase diagram in Figure 3 and tabulated in Table I. The discrepancy between samples was 3-4 K.

The experimentally determined solidus is much flatter than was previously reported. Although other systems, such as NaCl-KCl ⁹ or PbS-PbTe ¹⁰, have remarkably flat solidus boundaries between solid and liquid solutions, a horizontal solidus may indicate a eutectic with limited solid solution. To investigate this possibility we prepared samples which are known to form a eutectic with limited solid solution of KNO_3 (e.g., CsNO_3 and KNO_3 ¹¹),

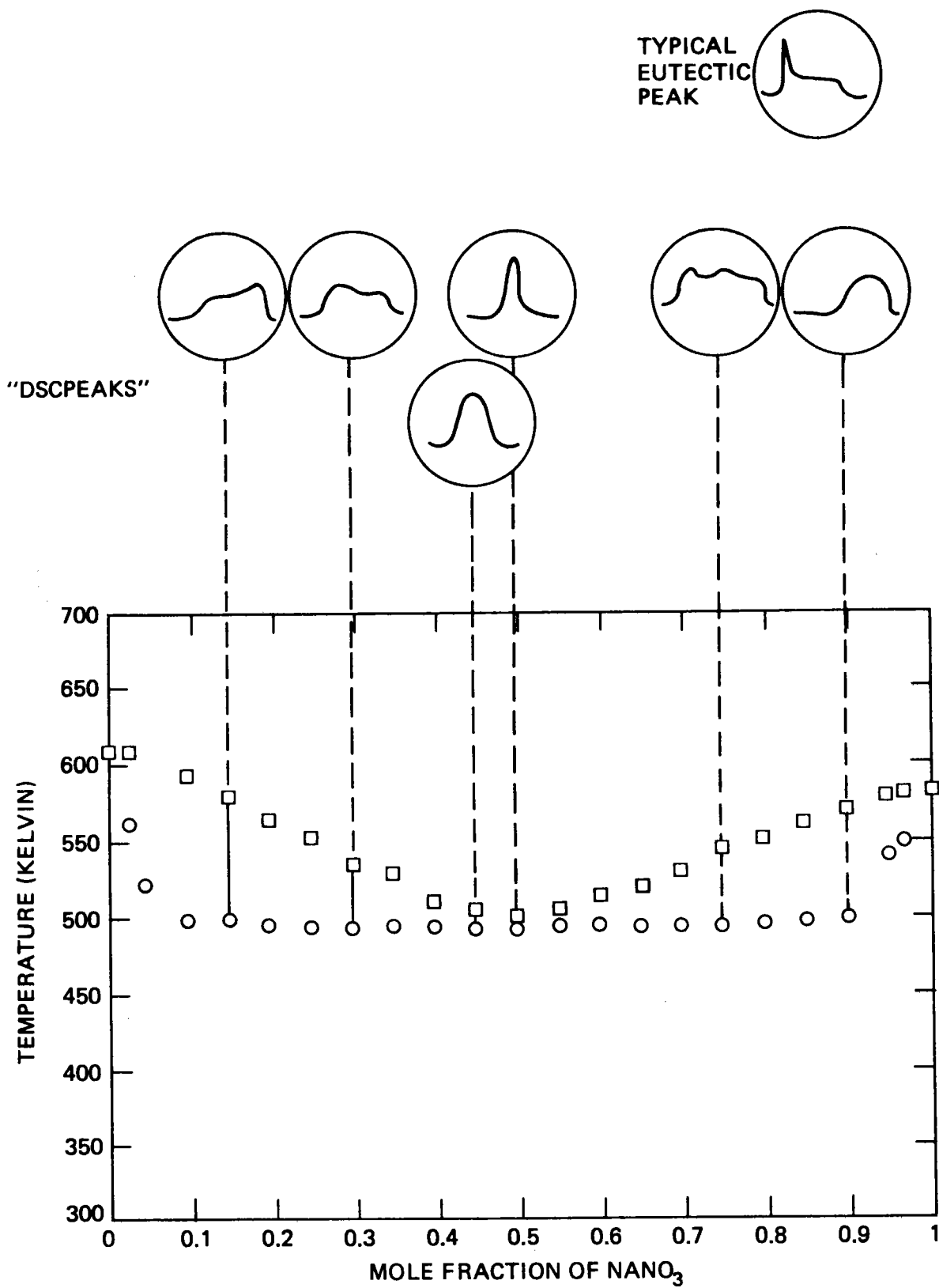


Fig. 2: The various DCS peaks for different $\text{NaNO}_3\text{-KNO}_3$ compositions shown with the solidus and liquidus data.

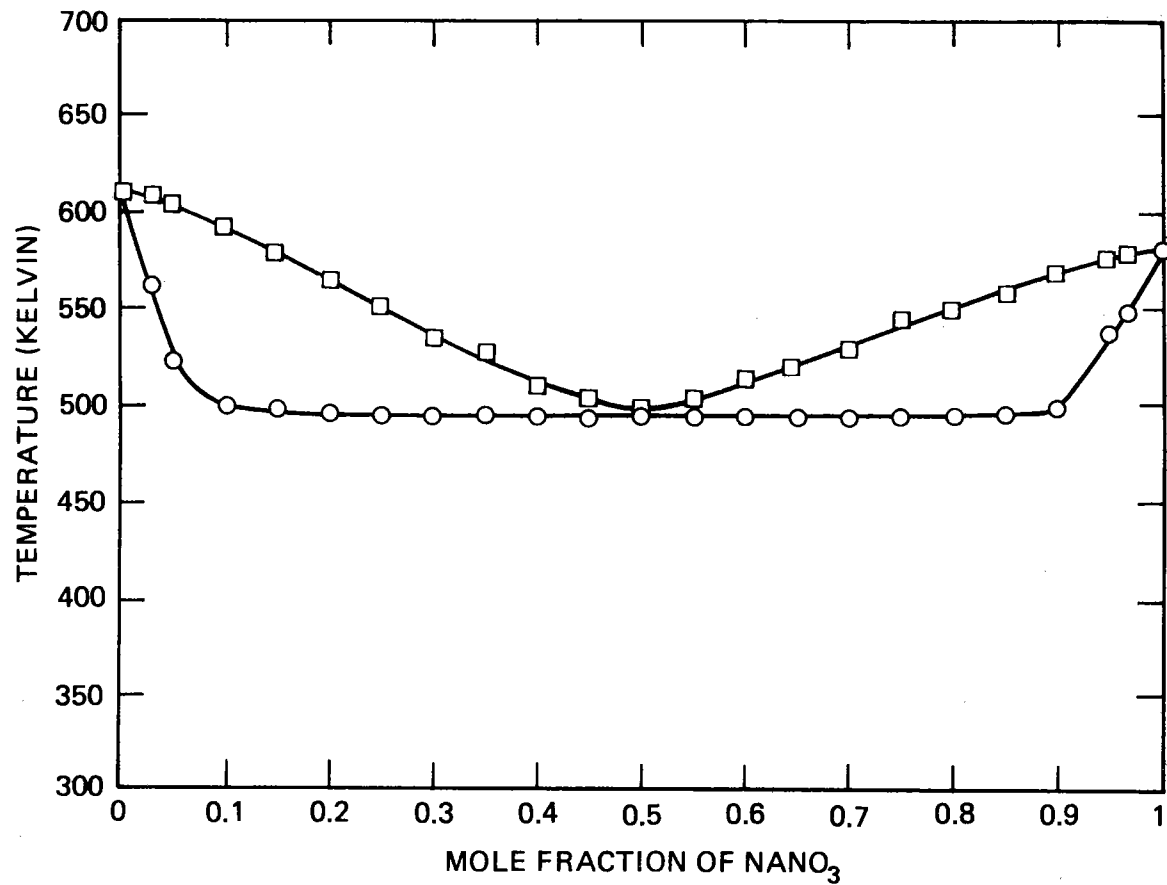


Fig. 3: Experimental DSC data for $\text{NaNO}_3\text{-KNO}_3$.
The points are connected for clarity.

TABLE I
DSC DATA FOR THE (Na/K)NO₃ SYSTEM

Mole Fraction NaNO ₃	Solidus Temperature (K)	Liquidus Temperature (K)
0.0	608.	608.
0.03	562.	608.
0.05	522.	605.
0.10	500.	592.
0.15	499.	578.
0.20	495.	564.
0.25	495.	552.
0.30	494.	535.
0.35	495.	528.
0.4	494.	510.
0.45	493.	505.
0.50	494.	500.
0.55	494.	505.
0.60	494.	514.
0.65	494.	520.
0.70	494.	529.
0.75	494.	545.
0.80	495.	550.
0.85	497.	558.
0.90	499.	568.
0.95	539.	577.
0.97	549.	580.
1.	580.	580.

determined their DSC peaks, and compared these with the $\text{NaNO}_3/\text{KNO}_3$ results. The DSC peaks observed in the vicinity of the eutectic were not the same shape as those observed for the $\text{NaNO}_3\text{-KNO}_3$. Rather, the DSC traces had the more classic peak shape described in Reference 12 and sketched in Figure 2 for eutectic systems. One can visualize the situation where the solidus is nearly horizontal by studying Figure 4, which schematically represents the free energy as a function of composition at the minimum melting temperature.

The flat solidus also led us to suspect that there may have been some contamination of the samples, such as due to water. To check this possibility we exposed several samples to high humidity. These samples had lower liquidus temperatures than did carefully dried samples, a fact which agrees with the trends in the $\text{KNO}_3/\text{NaNO}_3/\text{H}_2\text{O}$ ternary reported by Bergman and Shulyak.¹⁷ We also checked our DSC samples for contamination from reaction with the air or decomposition. An IR spectrum was made of a DSC sample that had been repetitively cycled to high temperature. No decomposition or reaction with air or water was observed. Inspection of used pans showed that no evidence of a reaction between the salts and pans.

Phase transformations of pure NaNO_3 and KNO_3 have been studied in great detail¹³⁻¹⁶ and are reviewed in Reference 13. At 548.5 K sodium nitrate transforms from an ordered rhombohedral phase to a disordered rhombohedral structure. Potassium nitrate is orthorhombic at room temperature but undergoes a phase transformation at 403 K to a rhombohedral structure to become isostructural with NaNO_3 . On cooling, however, KNO_3 usually reverts to the orthorhombic phase via an intermediate and slightly less symmetric rhombohedral phase that exists from 383 to 397 K. Rao et al.¹³ regard this form as metastable at the temperatures and pressures studied here, but they suggest it may appear in DSC experiments. Indeed, we did observe small DSC

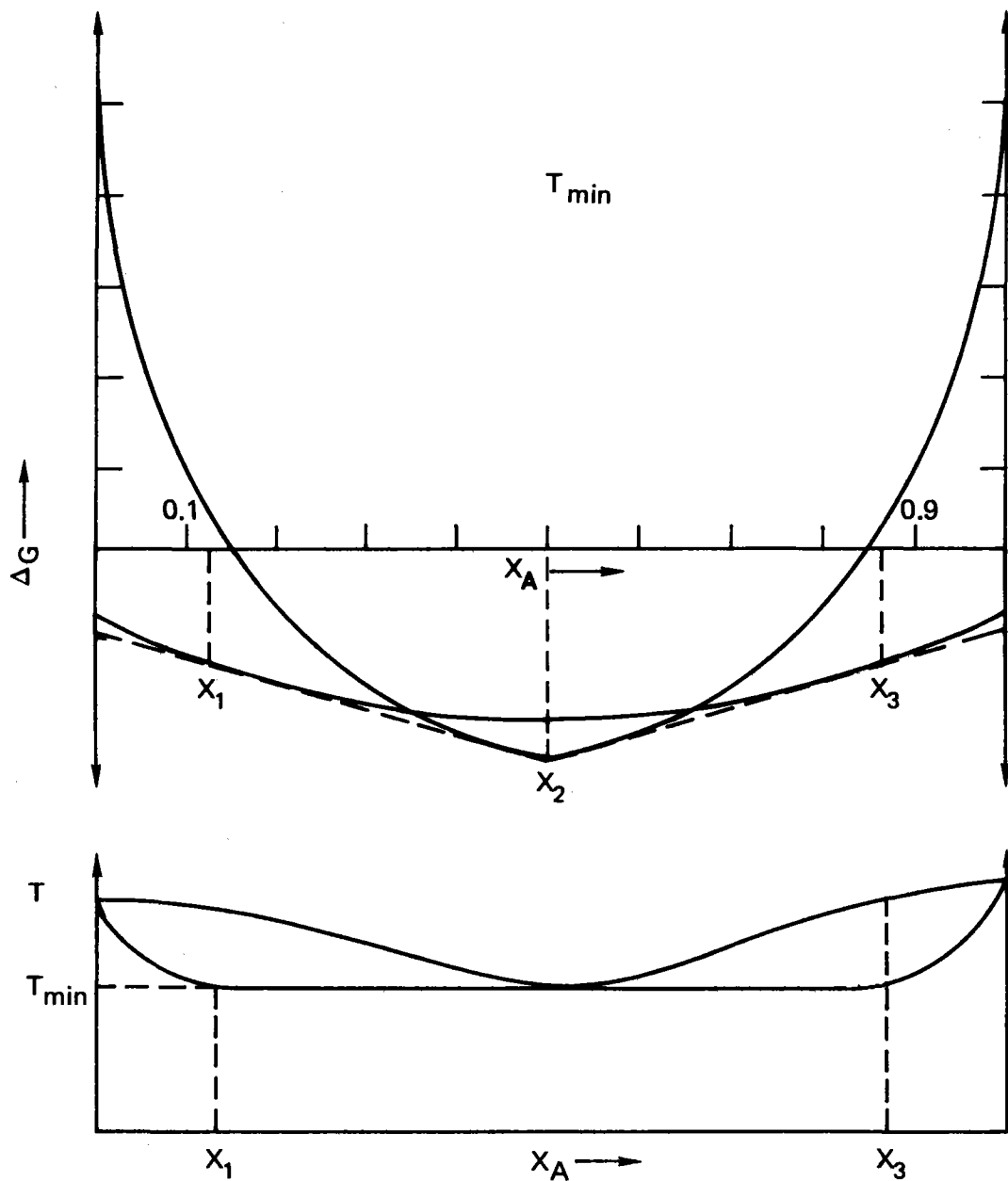


Fig. 4: A relationship between the free energy curves of solid and liquid solutions that could cause a very flat solidus in a binary solution.

peaks at ~385 K or ~400 K in KNO_3 containing mixtures. The temperature was dependent upon composition and pretreatment of the samples.

Investigating the minimum temperature phenomenon further, we analyzed several DSC samples by powder x-ray diffraction to seek evidence of solid solution formation of NaNO_3 - KNO_3 , such as is found in the pure substances. However, although we quenched NaNO_3 and KNO_3 mixtures from above and below the liquidus, two distinct and sharp crystal patterns were always obtained for rhombohedral NaNO_3 and orthorhombic KNO_3 by x-ray diffraction. No homogenous patterns for a NaNO_3 / KNO_3 solid rhombohedral solution were observed. Rhombohedral KNO_3 could not be quenched into the samples. We feel that a technique such as high temperature x-ray diffraction is necessary to observe the solid solution.

Theory

The behavior of binary systems of molten salts having a common anion has received considerable theoretical attention.¹⁸⁻²¹ Examining his measurements of heat of mixing of liquid NaNO_3 and KNO_3 , Kleppa²¹ found that regular solution theory applies. Measurements of the surface tension²² of 50/50 (Na/K) NO_3 are agree well with calculations using the measured heat of mixing and substantiate the applicability of regular solution theory to this system of salts.

A regular solution is a mixture that deviates from ideal solution behavior in a simple manner. The entropy of several components mixed to form a regular solution is purely configurational, as with ideal solutions:

$$\Delta S_{\text{mix}} = X_A \ln X_A + X_B \ln X_B \quad (1)$$

Regular solutions have a nonzero enthalpy of mixing, and an often-used form is

$$\Delta H_{\text{mix}} = X_A X_B (a + bX_A + cX_A X_B), \quad (2)$$

where X_A is the mole fraction of the component having the smaller size ($A = \text{NaNO}_3$ in this case) and a , b , and c are empirical constants. As derived from calorimetric studies²¹ of liquid solutions of NaNO_3 and KNO_3 (618-723 K) the values of a , b , and c are -408., -68., and ~0. cal/mole.

One can express the thermodynamic equilibrium of a solid solution and a liquid solution of A and B as sketched in Figure 5. The overall free energy of the reaction $A_{\text{SS}} = A_{\text{LS}}$ must be zero because the solid and liquid solutions are at equilibrium. From Figure 5 we see that the free energy of the overall reaction for component A ($A_{\text{SS}} = A_{\text{LS}}$) may be expressed as

$$\Delta G \equiv 0 = \begin{array}{l} \text{(i)} \quad \text{(ii)} \quad \text{(iii)} \\ (\Delta H_A - T\Delta S_A) + (\overline{\Delta H}_{\text{mix}}^A - T\overline{\Delta S}_{\text{mix}}^A) - (\overline{\Delta H}_{\text{mix}}^A - T\overline{\Delta S}_{\text{mix}}^A) \end{array} \quad (3)$$

The expressions ΔH_A and ΔS_A are the enthalpy and entropy of melting component A . The partial enthalpies and entropies of mixing in either the solid or the liquid solution are given by $\overline{\Delta H}_{\text{mix}}^A$ and $\overline{\Delta S}_{\text{mix}}^A$.

Equation (3) can be evaluated when assumptions and substitutions are made. Expression (i) is simply the free energy of fusion of component A at some temperature other than the melting point (where it is zero). The terms in (i) are corrected for temperature variations by

$$\Delta H_A = \Delta H^\circ - \int_T^{T_{\text{MP}}} (C_{pL} - C_{pS}) dT \quad (4)$$

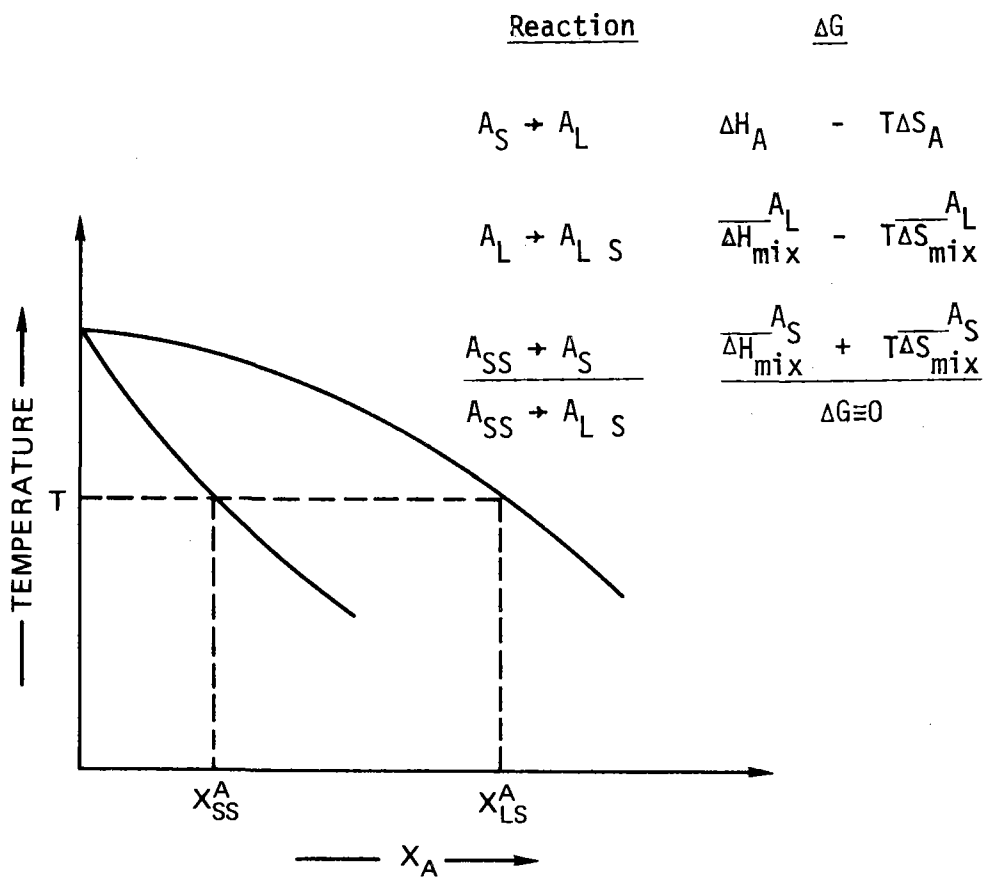


Fig. 5: Section of a general binary phase diagram.

A solid solution x_{SS}^A is in equilibrium with a liquid solution x_{LS}^A at temperature T ; therefore, the free energy of the reaction is 0.

For $A_S \rightarrow A_L$, ΔH_A and ΔS_A refer to the melting of component A. For $A_L \rightarrow A_{LS}$ and $A_{SS} \rightarrow A_S$, ΔH and ΔS refer to the partial molar quantities for mixing A.

$$\Delta S_A = \Delta S^\circ - \int_T^{T_{MP}} \frac{(C_{pL} - C_{pS})}{T} dT \quad (5)$$

where T_{MP} is the melting point of component A, and ΔH_A° and ΔS_A° are the enthalpy and entropy of fusion of A at its melting point. The correction terms arise from the difference in heat capacities between the solid (C_{pS}) and the liquid (C_{pL}).²³

In order to evaluate (ii) and (iii), both the solid and liquid solutions are assumed to exhibit regular solution behavior. The partial molar enthalpy of mixing for component A, $\overline{\Delta H}_{mix}^A$ or $\overline{\Delta H}_{mix}^L$ (in the solid or liquid solution, respectively), may then be found by applying to Eq. (2) the Gibbs-Duhem equation,

$$\overline{\Delta H}_{mix}^A = \Delta H_{mix} - x_B \frac{d \Delta H_{mix}}{dx_B} \quad (6)$$

The value of $\overline{\Delta H}_{mix}^L$ can be found explicitly from Kleppa's values.²¹ A similar equation can be written for the equilibrium of component B in both the solid and liquid solutions. The differences between the equations for components A and B are introduced by the asymmetry factor b in the enthalpies of mixing and are carried through the Gibbs-Duhem equation to obtain $\overline{\Delta H}_{mix}^A$ and $\overline{\Delta H}_{mix}^B$, the partial molar enthalpies of mixing.

Substituting Eqs. (1), (2), and (4)-(6) into (3) results in two nonlinear equations in T and x_A or x_B . A computer routine was written to simultaneously solve the two forms of (3) for NaNO_3 and KNO_3 . The routine incorporated a library algorithm based on an iterative variation of Newton's method and Gaussian elimination in a manner similar to the Gauss-Seidel process.²⁴ The program was supplied with the values from Reference 21 for a and b in the

enthalpy of mixing of liquid solutions (c was assumed to be zero) and the appropriate values from Reference 25 of C_{pL} , C_{pS} , ΔH° and ΔS° for NaNO_3 and KNO_3 . The value of a for the solid solution was systematically increased until the minimum melting point that was calculated coincided with the experimentally determined minimum melting point. For $\text{NaNO}_3\text{-KNO}_3$ solid solutions the value of $a = + 1500 \text{ cal/mole}$ gave the correct minimum melting point. Changing a from $\frac{1400 \text{ cal}}{\text{mole}}$ to 1500 cal/mole lowered the minimum melting point from 500 K to 495 K . The value of b was then varied to try to improve the fit of the model to the experimental data. If b is decreased from 0 to -500 cal/mole , the minimum melting point location is shifted from 495 K at $x_{\text{NaNO}_3} = .483$ to 501 K at $x_{\text{NaNO}_3} = .453$. Because b is primarily an asymmetry factor (and the phase diagram was experimentally observed to be symmetric) the best fit was for $b = 0 \text{ cal/mole}$.

Calculational Results and Comparison with Experiment

Osculating phase boundaries are predicted for the equilibrium of solid and liquid solutions,²⁶ and were generated by the calculational routines. Figure 6 compares our data with the results of the computer program for $a = + 1500 \text{ cal/mole}$ and $b = 0 \text{ cal/mole}$ for solid solutions of $\text{NaNO}_3\text{/KNO}_3$. The expression for the enthalpy of mixing of the solid solutions is given by equation (7).

$$\Delta H_{\text{mix}}^{\text{ss}} = x_{\text{NaNO}_3} x_{\text{KNO}_3} (1500) \frac{\text{cal}}{\text{mole}} \quad (7)$$

The positive value of a for the solid solutions indicates a tendency towards clustering of like ions in the solid solutions.

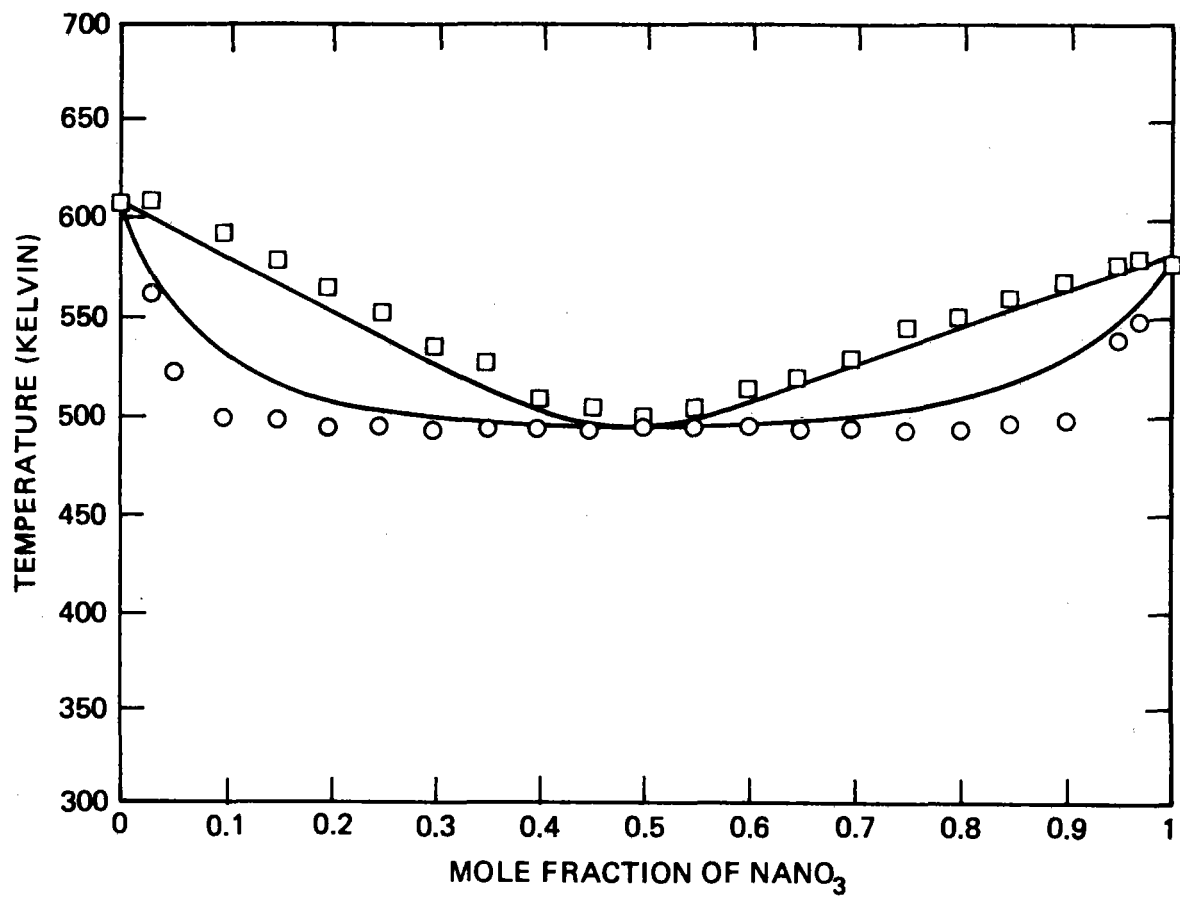


Fig. 6: Experimental data points and the calculated liquidus and solidus.

The calculated phase diagram is overlaid on the published phase diagrams in Figure 7. The liquidus determined in this work, the previously reported liquidus, and the liquidus from our model are in good agreement across the phase diagram. The solidus we determined experimentally is lower than the solidus from our model or previously determined solidus. The discrepancies are as large as 30 K between the previously determined solidus and the present work for the .1 and .9 mole fraction mixtures of NaNO₃ with KNO₃. We could not resolve this disagreement in the present and prior data. The experimentally determined solidus lies closer to the calculated phase diagram than to the published phase diagram. The calculated solidus is lower than the previously determined experimental solidus.

In our attempt to analytically describe the thermodynamics of NaNO₃-KNO₃ mixtures several assumptions and approximations were made. The mixing parameters, *a* and *b*, may be slightly temperature dependent, but this was neglected. Kleppa²¹ made his measurements of the enthalpy of mixing at higher temperatures (618-723 K) than the temperatures studied here (490-610 K).

For systems that deviate from randomness, alternative expressions have been defined²³ for the free energy of mixing, such as

$$\Delta G_{\text{mix}} = X_A X_B \left(1 - \frac{X_A X_B K}{ZRT} \right) - T \Delta S_{\text{mix}} \quad (6)$$

Here, *K* is a constant, *Z* is the coordination number, and *R* and *T* have their usual meanings. The value of *Z* was estimated to be 5 based on Reference 27. This form for the free energy of mixing was incorporated into the computer program to calculate the phase diagram, and a number of values

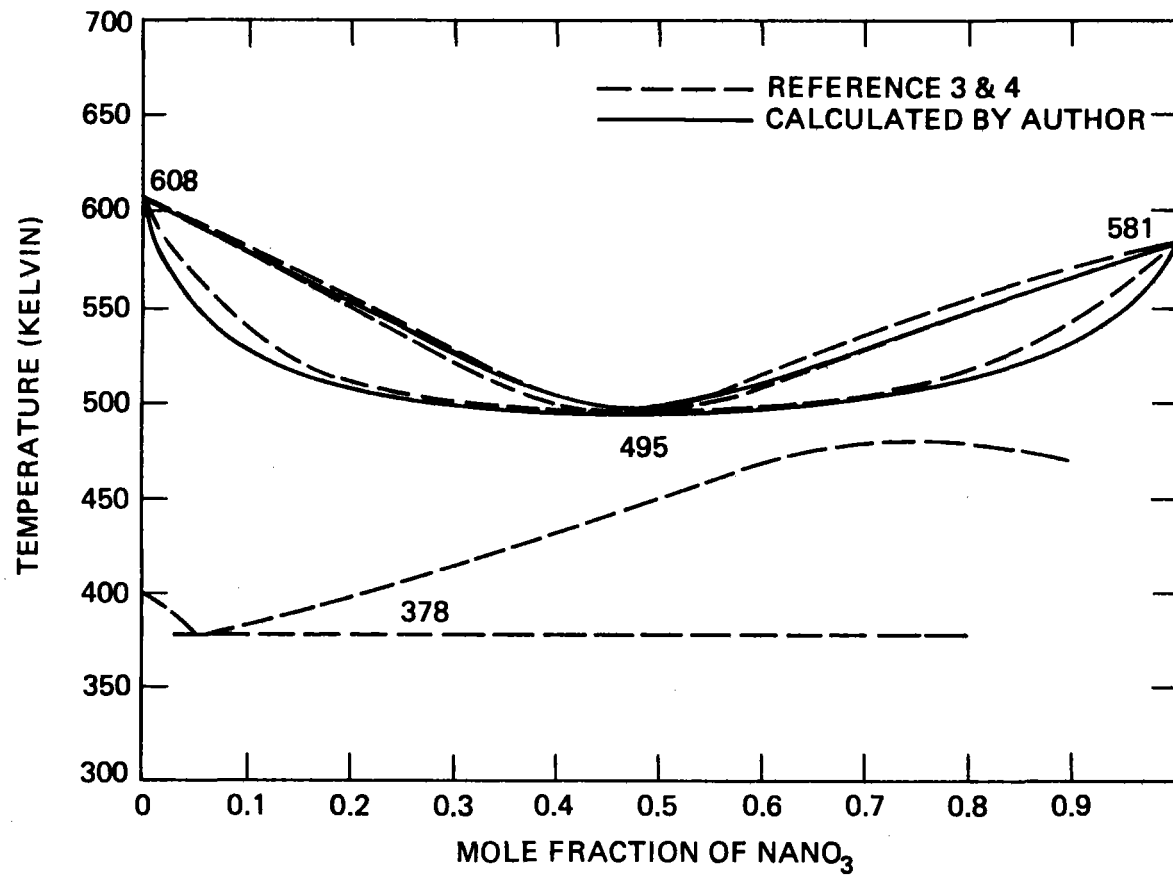


Fig. 7: The calculated solidus and liquidus overlaid with the previously published phase diagram.

of K ranging from 0 to 2000 cal/mole were tried. The results were similar to the regular solution treatment and the solidus was not flatter. Although a more elaborate description of the excess entropy contributions--such as using Legendre polynomials⁶--may contribute to the accuracy in describing the NaNO₃/KNO₃ thermodynamics, we did not explore that possibility.

NaCl-KCl Calculations

As verification of the validity of the computer program, it was applied to NaCl/KCl, a system homologous to NaNO₃/KNO₃. The mixing parameters for liquid solutions have been determined to be $a_L = -490$ cal/mole and $b_L = -65$ cal/mole.¹⁸ Tobolsky²⁸ calculated the enthalpy of mixing for a solid solution of 50/50 NaCl/KCl to be 1188 cal/mole. We assumed that the solid solutions would exhibit regular solution behavior and that the asymmetry factor b was zero for the solid solutions of NaCl/KCl. Therefore, using Eq. (2), a_S is 4(1188) cal/mole or 4752 cal/mole. This value of a_S and the above values of a_L and b_L were used in calculations of the NaCl/KCl phase diagram (see Figure 8). The resulting liquidus and solidus had a minimum melting point of 880 K, which is within about 4% of a recent experimental determination,⁹ (918 K). The experimental minimum melting point can be obtained exactly by changing the value of a_S to 3200. cal/mole. The corresponding heat of mixing of solid 50/50 (Na/K)Cl is then 800 cal/mole. Tobolsky pointed out that the value of his heat of mixing of solid NaCl/KCl was approximate; therefore, a value of 800 cal/mole may be considered very reasonable.

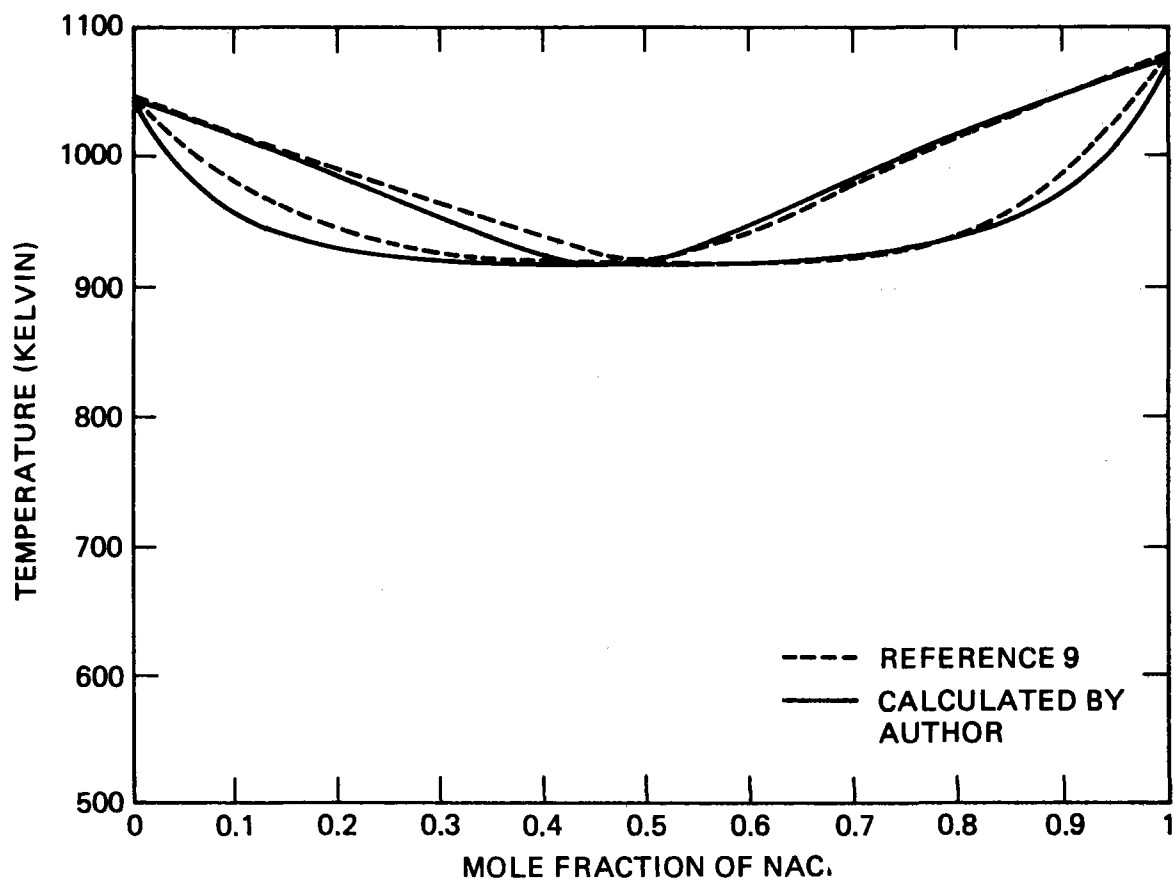


Fig. 8: Calculated and experimental phase diagrams for NaCl-KCl.

Conclusions

The phase diagram of $\text{NaNO}_3/\text{KNO}_3$ was studied using differential scanning calorimetry. The solidus was determined to be flatter than previously reported. A computer code was developed from regular solution theory and thermodynamics that approximated the experimental data. Using the code we estimated the heat of mixing of the solid solution to be 375 cal/mole for an equimolar mixture of NaNO_3 and KNO_3 . The computer code was also successfully applied to the NaCl/KCl phase diagram. In contrast to the previously reported value of 1188. cal/mole, the heat of mixing of 50/50 (Na/K)Cl was calculated to be 800. cal/mole. For future work on more complex systems, the results of this study can serve as a suitable starting point.

ACKNOWLEDGMENTS

We would like to thank Joanne Volponi (8313) for her technical assistance with the DSC and Bob Tucker for his work in editing this report. Thanks also to Dale Boehme (8313) for his x-ray analysis and Cal Feemster (8315) for the IR analysis.

REFERENCES

1. L. Radosevich, "Thermal Energy Storage for Advanced Solar Central Receiver Power Systems," Sandia Laboratories, report SAND78-8221 (1978).
2. L. Tallerico, "A Description and Assessment of Large Solar Power Systems Technology," Sandia Laboratories report SAND79-8015 (1979).
3. A. G. Bergman and S.I. Berul, Izvest. Sektora Fiz. - Khim. Anal., Inst. Obshehei Neorg. Khim., Akad. Nauk SSSR 21, 178-83 (1952).
4. A. Kofler, Montash. 86, 643-52 (1955).
5. Handbook of Solid-Liquid Equilibria in Systems of Anhydrous Inorganic Salts, V1, edited by N. K. Voskresenskaya, (Keter Press, 1970).
6. P. L. Lin, A. D. Pelton, and C. W. Bale, J. Amer. Ceram. Soc. 62 (7-8), 414 (1979).
7. L. Kaufman, Computer Calculations of Phase Diagrams, (Acad. Pr., NY, 1970).
8. A. P. Gray, "A Brief study of the Phase Behavior of KNO₃ in a Differential Scanning Calormeter," Perkin Elmer Thermal Analysis Application Study, TAAS-1, P173, Norwalk, Connecticut.
9. D. S. Coleman and, P. D. A. Lacy, Mater. Res. Bull. 2 (10), 936 (1967).
10. M. S. Darrow, W. B. White, and R. Roy, Trans AIME 236 (5), 654 (1966).
11. L. A. Panieva, L. L. Gabitova, and P. I. Protsenko, Russ. J. Inorg. Chem. 13 (10) 1450 (1968).
12. R. L. Fyans, "Determination of the Phase Behavior of Alloys by Differential Scanning Calorimetry," Instrument News 21 (1), Perkin Elmer Corporation, Norwalk, Conn.
13. C. N. R. Rao, B. Prakat, and M. Natarajan, Nat. NSRDS-NBS53, May (1975).
14. E. R. Johnson, A. Frances, and C. C. Wu, J. App. Phys. 47, (5) 1827 (1976).
15. F. C. Kracek, J. Amer. Chem. Soc., 53, (7) 2609 (1931).
16. F. C. Kracek, E. Posnjak, and S. B. Hendricks, J. Am. Chem. Soc. 53, (9) 3339 (1931).
17. A. G. Bergman and L. F. Shulyak, Russ J. of Inorg. Chem. 18, (5) 731 (1973).

18. L. S. Hersh and O. J. Kleppa, J. Chem. Phys. 42, (4) 1309 (1965).
19. O. J. Kleppa, R. B. Clarke, and L. S. Hersh, J. Chem. Phys. 35, (7), 175 (1961).
20. O. J. Kleppa and L. S. Hersh, J. Chem. Phys. 34, (2) 351 (1961).
21. O. J. Kleppa, J. Phys. Chem. 64 1937 (1960).
22. D. A. Nissen and B. H. Van Domelan, J. Chem. Phys. 79, 2003 (1975).
23. R. A. Swalin, Thermodynamics of Solids (J. Wiley & Sons, New York, 1972) Chapter 7.
24. K. H. Haskell and R. E. Jones, Sandia Laboratories report SAND77-1441 (1977).
25. I. Barin and O. Knacke, Thermochemical Properties of Inorganic Substances (Springer-Verlag, Berlin, 1973).
26. C. Wagner, ACTA met. 2, (2) 242 (1954).
27. Molten Salt Chemistry, edited by M. Blander, (Interscience Pub.) p. 164.
28. A. V. Tobolsky, J. Chem. Phys. 10, 187 (1942).

UNLIMITED RELEASE

INITIAL DISTRIBUTION

R. A. Higgins
Dept. of Materials Science and Engineering
Stanford University
Stanford, CA 94305

G. Mamantov
Department of Chemistry
University of Tennessee
Knoxville, TN 37916

Z. A. Munir
Department of Mechanical Engineering
UC Davis
Davis, CA 94616

S. L. Roche
Lawrence Berkeley Laboratory
Building 62
Berkeley, CA 94720

J. N. Sweet, 5824
R. J. Eagan, 5845
R. P. Clark, 25
E. Beauchamp, 5846
T. B. Cook, 8000; Attn: A. N. Blackwell, 8200
B. F. Murphey, 8300
R. L. Rinne, 8320
G. W. Anderson, 8330
W. Bauer, 8340
D. L. Hartley, 8350
D. M. Schuster, 8310
A. J. West, 8312
C. M. Kramer, 8313 (20)
A. S. Nagelberg, 8313
D. A. Nissen, 8313
J. V. Volponi, 8313 (5)
C. J. Wilson, 8313 (10)
R. W. Mar, 8313
W. R. Hoover, 8314
L. A. West, 8315
J. Swearengen, 8316
L. Gutierrez, 8400
W. Wilson, 8453
L. Radosevich, 8453
A. C. Skinrood, 8452
R. W. Carling, 8453
Publications Division, 8265, for TIC (2)
8265/Technical Library Processes Division, 3141
Technical Library Processes Division, 3141 (2)
Library and Security Classification Division, 8266 (3)

